Wide-field imaging of fluorescent deoxy-glucose in e*x vivo* malignant and normal breast tissue

R. J. Langsner,[1,*] L. P. Middleton,[2] J. Sun,[3] F. Meric-Bernstam,[4,5] K. K. Hunt,[4,6,] R. A. Drezek,[1,7,9] and T. K. Yu[8,9]

[1]*Department of Bioengineering, Rice University, 6100 Main St. Houston, Texas 77005, USA*
[2]*Department of Pathology, University of Texas, M.D. Anderson Cancer Center, 1515 Holcombe Blvd., Houston, Texas 77030, USA*
[3]*Suzhou Institute of Biomedical Engineering and Technology, Chinese Academy of Sciences, Suzhou New District, China, 215163, China*
[4]*Department of Surgical Oncology, University of Texas, M.D. Anderson Cancer Center, 1515 Holcombe Blvd., Houston, Texas 77030, USA*
[5]*Program in Cancer Biology, University of Texas Graduate School of Biomedical Sciences at Houston, P.O. Box 20334 Houston, Texas 77225, USA*
[6]*Department of Experimental Radiation Oncology, University of Texas, M.D. Anderson Cancer Center, 1515 Holcombe Blvd., Houston, Texas 77030, USA*
[7]*Department of Electrical and Computer Engineering, Rice University, 6100 Main St. Houston, TX 77005, USA*
[8]*Houston Precision Cancer Center, 10405 Katy Freeway, Houston, TX 77024*
[9]*These authors contributed equally to this work.*
rl9@rice.edu

Abstract: Rapid in situ determination of surgical resection margins during breast cancer surgery would reduce patient time under anesthesia. We present preliminary data supporting the use of a fluorescent glucose analog (2-NBDG) as an optical contrast agent to differentiate freshly excised breast tissue containing cancerous cells from normal breast tissue. Multi-spectral images of 14 breast cancer specimens acquired before and after incubation with 2-NBDG demonstrated increased fluorescent signal in all of the malignant tissue due to increased 2-NBDG consumption. We demonstrate that 2-NBDG has potential as an optical contrast agent to differentiate cancerous from non-cancerous tissue.

OCIS Codes: (170.1610) Clinical applications; (170.3880) Medical and biological imaging.

References and links

1. N. Q. Mirza, G. Vlastos, F. Meric, T. A. Buchholz, N. Esnaola, S. E. Singletary, H. M. Kuerer, L. A. Newman, F. C. Ames, M. I. Ross, B. W. Feig, R. E. Pollock, M. McNeese, E. Strom, and K. K. Hunt, "Predictors of locoregional recurrence among patients with early-stage breast cancer treated with breast-conserving therapy," Ann. Surg. Oncol. **9**(3), 256–265 (2002).
2. A. Luini, J. Rososchansky, G. Gatti, S. Zurrida, P. Caldarella, G. Viale, G. Rosali dos Santos, and A. Frasson, "The surgical margin status after breast-conserving surgery: discussion of an open issue," Breast Cancer Res. Treat. **113**(2), 397–402 (2009).
3. L. R. Bickford, G. Agollah, R. Drezek, and T. K. Yu, "Silica-gold nanoshells as potential intraoperative molecular probes for HER2-overexpression in ex vivo breast tissue using near-infrared reflectance confocal microscopy," Breast Cancer Res. Treat. **120**(3), 547–555 (2010).
4. L. P. Adler, P. F. Faulhaber, K. C. Schnur, N. L. Al-Kasi, and R. R. Shenk, "Axillary lymph node metastases: screening with [F-18]2-deoxy-2-fluoro-D-glucose (FDG) PET," Radiology **203**(2), 323–327 (1997).
5. M. Schelling, N. Avril, J. Nährig, W. Kuhn, W. Römer, D. Sattler, M. Werner, J. Dose, F. Jänicke, H. Graeff, and M. Schwaiger, "Positron emission tomography using [(18)F]Fluorodeoxyglucose for monitoring primary chemotherapy in breast cancer," J. Clin. Oncol. **18**(8), 1689–1695 (2000).
6. R. L. Wahl, R. L. Cody, G. D. Hutchins, and E. E. Mudgett, "Primary and metastatic breast carcinoma: initial clinical evaluation with PET with the radiolabeled glucose analogue 2-[F-18]-fluoro-2-deoxy-D-glucose," Radiology **179**(3), 765–770 (1991).
7. O. Warburg, F. Wind, and E. Negelein, "The metabolism of tumors in the body," J. Gen. Physiol. **8**(6), 519–530 (1927).
8. L. P. Adler, J. P. Crowe, N. K. al-Kaisi, and J. L. Sunshine, "Evaluation of breast masses and axillary lymph nodes with [F-18] 2-deoxy-2-fluoro-D-glucose PET," Radiology **187**(3), 743–750 (1993).

#145022 - $15.00 USD Received 30 Mar 2011; revised 2 May 2011; accepted 10 May 2011; published 11 May 2011

9. R. S. Brown, J. Y. Leung, P. V. Kison, K. R. Zasadny, A. Flint, and R. L. Wahl, "Glucose transporters and FDG uptake in untreated primary human non-small cell lung cancer," J. Nucl. Med. **40**(4), 556–565 (1999).
10. R. S. Brown and R. L. Wahl, "Overexpression of Glut-1 glucose transporter in human breast cancer. An immunohistochemical study," Cancer **72**(10), 2979–2985 (1993).
11. G. Weber and A. Cantero, "Glucose-6-phosphatase activity in normal, pre-cancerous, and neoplastic tissues," Cancer Res. **15**(2), 105–108 (1955).
12. K. Yu, S. J. Schomisch, V. Chandramouli, and Z. Lee, "Hexokinase and glucose-6-phosphatase activity in woodchuck model of hepatitis virus-induced hepatocellular carcinoma," Comp. Biochem. Physiol. Part Toxicol. Pharmacol. **143**(2), 225–231 (2006).
13. K. Yamada, M. Nakata, N. Horimoto, M. Saito, H. Matsuoka, and N. Inagaki, "Measurement of glucose uptake and intracellular calcium concentration in single, living pancreatic beta-cells," J. Biol. Chem. **275**(29), 22278–22283 (2000).
14. R. G. O'Neil, L. Wu, and N. Mullani, "Uptake of a fluorescent deoxyglucose analog (2-NBDG) in tumor cells," Mol. Imaging Biol. **7**(6), 388–392 (2005).
15. N. Nitin, A. L. Carlson, T. Muldoon, A. K. El-Naggar, A. Gillenwater, and R. Richards-Kortum, "Molecular imaging of glucose uptake in oral neoplasia following topical application of fluorescently labeled deoxy-glucose," Int. J. Cancer **124**(11), 2634–2642 (2009).
16. A. Fourquet, F. Campana, B. Zafrani, V. Mosseri, P. Vielh, J. C. Durand, and J. R. Vilcoq, "Prognostic factors of breast recurrence in the conservative management of early breast cancer: a 25-year follow-up," Int. J. Radiat. Oncol. Biol. Phys. **17**(4), 719–725 (1989).
17. M. C. Smitt, K. Nowels, R. W. Carlson, and S. S. Jeffrey, "Predictors of reexcision findings and recurrence after breast conservation," Int. J. Radiat. Oncol. Biol. Phys. **57**(4), 979–985 (2003).
18. S. C. Renton, J. C. Gazet, H. T. Ford, C. Corbishley, and R. Sutcliffe, "The importance of the resection margin in conservative surgery for breast cancer," Eur. J. Surg. Oncol. **22**(1), 17–22 (1996).
19. C. A. Perez, "Conservation therapy in T1-T2 breast cancer: past, current issues, and future challenges and opportunities," Cancer J. **9**(6), 442–453 (2003).
20. M. E. Peterson, D. J. Schultz, C. Reynolds, and L. J. Solin, "Outcomes in breast cancer patients relative to margin status after treatment with breast-conserving surgery and radiation therapy: the University of Pennsylvania experience," Int. J. Radiat. Oncol. Biol. Phys. **43**(5), 1029–1035 (1999).
21. R. Heimann, C. Powers, H. J. Halpern, A. G. Michel, C. A. Ewing, B. Wyman, W. Recant, and R. R. Weichselbaum, "Breast preservation in stage I and II carcinoma of the breast. the University of Chicago experience," Cancer **78**(8), 1722–1730 (1996).
22. R. Bos, J. J. M. van Der Hoeven, E. van Der Wall, P. van Der Groep, P. J. van Diest, E. F. Comans, U. Joshi, G. L. Semenza, O. S. Hoekstra, A. A. Lammertsma, and C. F. Molthoff, "Biologic correlates of (18)fluorodeoxyglucose uptake in human breast cancer measured by positron emission tomography," J. Clin. Oncol. **20**(2), 379–387 (2002).
23. N. Avril, M. Menzel, J. Dose, M. Schelling, W. Weber, F. Jänicke, W. Nathrath, and M. Schwaiger, "Glucose metabolism of breast cancer assessed by 18F-FDG PET: histologic and immunohistochemical tissue analysis," J. Nucl. Med. **42**(1), 9–16 (2001).
24. N. Y. Tse, C. K. Hoh, R. A. Hawkins, M. J. Zinner, M. Dahlbom, Y. Choi, J. Maddahi, F. C. Brunicardi, M. E. Phelps, and J. A. Glaspy, "The application of positron emission tomographic imaging with fluorodeoxyglucose to the evaluation of breast disease," Ann. Surg. **216**(1), 27–34 (1992).
25. R. Bos, J. J. M. van Der Hoeven, E. van Der Wall, P. van Der Groep, P. J. van Diest, E. F. Comans, U. Joshi, G. L. Semenza, O. S. Hoekstra, A. A. Lammertsma, and C. F. Molthoff, "Biologic correlates of (18)fluorodeoxyglucose uptake in human breast cancer measured by positron emission tomography," J. Clin. Oncol. **20**(2), 379–387 (2002).
26. A. M. Byrne, A. D. K. Hill, S. J. Skehan, E. W. McDermott, and N. J. O'Higgins, "Positron emission tomography in the staging and management of breast cancer," Br. J. Surg. **91**(11), 1398–1409 (2004).
27. O. E. Nieweg, E. E. Kim, W. H. Wong, W. F. Broussard, S. E. Singletary, G. N. Hortobagyi, and R. S. Tilbury, "Positron emission tomography with fluorine-18-deoxyglucose in the detection and staging of breast cancer," Cancer **71**(12), 3920–3925 (1993).
28. L. Arnould, M. Gelly, F. Penault-Llorca, L. Benoit, F. Bonnetain, C. Migeon, V. Cabaret, V. Fermeaux, P. Bertheau, J. Garnier, J. F. Jeannin, and B. Coudert, "Trastuzumab-based treatment of HER2-positive breast cancer: an antibody-dependent cellular cytotoxicity mechanism?" Br. J. Cancer **94**(2), 259–267 (2006).
29. S. F. Dent, S. Verma, K. I. Pritchard, J. Latreille, D. Rayson, M. Clemons, J. R. Mackey, L. Provencher, S. Verma, J. Lemieux, S. Chia, and B. Wang, "The role of her2-targeted therapies in women with her2-overexpressing metastatic breast cancer," Curr. Oncol. **16**(4), 25–35 (2009).

1. Introduction

Local recurrence of breast cancer after breast conservation therapy (BCT) can be influenced by a variety of risk factors such as age, tumor size, lymph node status, and tumor margins [1,2]. Positive margin status, in which malignant cells are present at the resection edge, is determinative in prognosis and adjuvant therapy planning. Positive margins often result in a

#145022 - $15.00 USD Received 30 Mar 2011; revised 2 May 2011; accepted 10 May 2011; published 11 May 2011

return to the operating room for additional resection and addition of higher dose radiation treatments. In many tertiary care centers, appropriate facilities and staff exist to allow assessment of margin status intraoperatively. Surgeons in these centers have the opportunity to remove more tissue during the same procedure to achieve negative margins if the initial resection margin is positive. However, many hospitals and smaller surgery suites in the general community do not have pathology support services to allow for intraoperative margin assessment, and thus the margin status is not known until several days after the surgery [3]. If positive margins are revealed, patients face the additional risks and costs of a second procedure, anxiety, and reduced probability of optimal cosmesis. Therefore, new methods to expedite intraoperative assessment of surgical margins are essential.

Positron Emission Tomography (PET) is currently being used in clinics to stage breast cancer and monitor response to therapy [4–6]. It utilizes a positron emitter analogue of glucose, 2-(fluorine-18)-(fluoro-2-deoxyglucose) (^{18}FDG) to monitor *in vivo* glucose uptake. PET leverages the higher metabolic state, higher expression of glucose transporters (GLUTs), and lower expression of glucose-6-phosphatase of malignant cells to image the high level of ^{18}FDG uptake in cancerous cells, distinguishing them from non-cancerous cells [7–12]. 2-[N-(7-nitrobenz-2-oxa-1, 3-diazol-4-yl)amino]-2-deoxy-d-glucose (2-NBDG) is a fluorescent glucose analogue that undergoes a similar pathway of uptake and metabolism to ^{18}FDG and accumulates preferentially in malignant cells [13,14]. In preclinical imaging studies, 2-NBDG accumulation was shown to be higher in cancerous cells than in normal cells [14,15]. Nitin et al. have demonstrated the use of 2-NBDG to enhance fluorescent molecular imaging of oral neoplasia [15].

In this study, we performed important proof of principle study that demonstrates that topical application of 2-NBDG can be used as an optical contrast agent to help differentiate cancerous tissue using a wide-field imaging system. We imaged fresh human breast tissue acquired from surgical specimens and stained them with 2-NBDG. We established that the 2-NBDG signal in tissue can be determined using a wide-field camera and filters to create multispectral images of tissue that can then be analyzed both qualitatively and semi-quantitatively by using the area under the curve metric of the spectral profile of the tissues. Our analysis demonstrated that 2-NBDG preferentially enhanced the fluorescent signal of malignant tissue. Future steps will be to develop a simpler and more portable wide-field optical system that uses 2-NBDG and can be used to assist in the detection of cancerous tissue at the resection site.

2. Materials and methods

2.1 2-NBDG characteristics

2-NBDG was acquired from Invitrogen in powdered form and was resuspended in 1X DPBS (Gibco) to a final concentration of 194 μM. The pH of the solution was 7.4. Aliquots of the fluorophore were kept frozen at −20°C in black centrifuge tubes until needed. Before receipt of the tissue, the aliquots were thawed in a 37°C water bath and kept at that temperature until being added to the specimens.

To evaluate variability in the imaging system in between testing days, 1 ml of 194 μM 2-NBDG was pipetted into a quartz cuvette and placed in the same position in the imaging system and imaged under the same conditions for four consecutive days. The spectra of each day was acquired and compared to determine the system's stability between testing days.

2.2 Ex vivo tissue acquisition

Freshly excised human breast tissue samples were acquired from 14 patients undergoing surgical resection of suspected breast cancer at The University of Texas MD Anderson Cancer Center with the approval of the institutional review boards at Rice University and MD Anderson. All patients gave written informed consent to participate. Each specimen was

#145022 - $15.00 USD Received 30 Mar 2011; revised 2 May 2011; accepted 10 May 2011; published 11 May 2011

received from surgery and inked so that the pathologist could identify the *in situ* location of the specimen. The specimen was then breadloafed in 2-5 mm increments and visually inspected and palpated to determine the area of residual tumor. Leftover specimen that was not necessary for diagnosis by the surgical pathologist was used for the imaging process. A separate specimen of normal tissue away from the gross tumor was also acquired as an internal control for each patient. For one patient (#2), a single specimen was obtained with gross palpable tumor at one end and normal appearing tissue at the other end. Typically, the tissues were processed for imaging within 60 minutes of resection.

2.3 Ex vivo tissue sampling

Upon receipt of the tissue, autofluorescent images of both normal and malignant tissue were acquired using a Maestro wide-field multispectral fluorescent camera (CRi, Woburn, MA). The imaging system has a spatial resolution of 25 μm/pixel and the field of view for each image acquired was 4.9 X 3.7 cm. The tissue samples were excited with filtered light (445-490 nm) and the emitted light was filtered (515 nm LP) before entering the camera. The exposure time for the camera was 18.56 ms. A multispectral image cube comprised of the different images at different wavelengths (520-720 nm, every 10 nm) was created using these settings. This process created a prestain image that would be used for comparison after the tissue had been stained with 2-NBDG.

After the prestain image cube was created, both normal and malignant tissue specimens were incubated topically with 2-NBDG at 37°C for 20 minutes in the dark. The remaining 2-NBDG was aspirated and the tissue samples were rinsed twice in cold PBS on ice in the dark for 10 minutes. The samples were placed under the wide-field camera in approximately the same positions as the prestain images. The tissues were subsequently imaged under the same conditions described above, and a poststain multispectral cube was created.

After imaging, the tissue samples were fixed in formalin for 24 hr, placed into 70% ethanol, and sent to the research pathology core laboratory at MD Anderson for hematoxylin-and-eosin (H&E) staining. Both the control and sample tissue slides were then reviewed by a breast pathologist (L.M.), who provided a histological diagnosis of the tissue. Pictures of the slides were taken at a 40X magnification using an Olympus DP70 camera (Center Valley, PA).

2.4 Fluorescence spectrum acquisition and quantitative analysis

For semi-quantitative analysis of the images, a region of interest (ROI) was custom-fit along the edges of the tissues on the before and after-staining images. The fluorescence spectrum from 520 to 720 nm of this ROI was plotted based on the fluorescent signal calculated at every 10 nm. The intensity for each wavelength was the average intensity for each pixel in the ROI. This allowed the creation of two sets of data for each of the tissues that could be used to compare the effect of adding 2-NBDG to both of the tissues. Tissue samples from one patient (#10) had only a data set for the post stain image due to a machine malfunction that was not detected until after the tissue had been stained; however, samples from this patient were included because poststain comparisons between the cancerous and noncancerous tissues could be made.

Analyses of each tissue spectrum revealed a slight peak in the 560-600 nm range for the prestain images and a larger, more prominent peak in the same range for the poststain images. To quantify the 2-NBDG signal from each tissue and compare the different samples, an area under the peak of each curve (AUC) was calculated by multiplying the height (fluorescent signal) of each curve at 580 nm by the width of the peak (40 nm). The area under the prestain curves was subtracted from that of the poststain curves to normalize the autofluorescence (NAUC). The average NAUC of the cancerous and normal tissue was calculated, as well, the mean of all samples was calculated. This mean was then drawn as a horizontal threshold line

#145022 - $15.00 USD Received 30 Mar 2011; revised 2 May 2011; accepted 10 May 2011; published 11 May 2011

to help discriminate between the two groups. Statistical significance between the groups of NAUCs was determined using a two-tailed Student's t-test.

The signal differences between the pre and poststain images at each wavelength from 520 to 720 nm were also calculated for each set of cancerous and normal tissues for the patients. For example, the differences at 580 nm for the cancerous tissue from each patient (excluding patient #10) were placed into one group and the differences at 580 nm for the normal control tissues were also placed into a group. The two groups were then compared by using a two-tailed student's t-test; this was done for each wavelength from 520 to 720 nm.

3. Results

3.1 Ex vivo tissue characteristics of freshly excised human breast tissue specimens

The pathologic diagnosis of each tissue sample was confirmed by a breast pathologist in a blinded fashion (Table 1). There were five tissues that contained invasive ductal carcinoma (IDC), one that contained invasive mammary carcinoma (IMC), three that contained invasive lobular carcinoma (ILC), three that contained ductal carcinoma in situ (DCIS), and two that contained no cancer cells. Of the two specimens that did not contain cancer cells, one was obtained (patient #13) from the periphery of resected breast tissue that did contain metaplastic carcinoma with both spindle cell and IDC components. The other tissue sample was from a patient (#14) who had received neoadjuvant chemotherapy and achieved a complete pathologic response. In that specimen, there was evidence of tissue repair and fibrosis.

Table 1. Patient and Sample Characteristics

Patient/Sample Number	Diagnosis	Nuclear Grade
1	Ductal Carcinoma in Situ	3
2	Ductal Carcinoma in Situ	3
3	Ductal Carcinoma in Situ	3
4	Invasive Ductal Carcinoma	2
5	Invasive Ductal Carcinoma	2
6	Invasive Ductal Carcinoma	2
7	Invasive Ductal Carcinoma	2
8	Invasive Ductal Carcinoma	2
9	Invasive Lobular Carcinoma	3
10	Invasive Lobular Carcinoma	3
11	Invasive Lobular Carcinoma	3
12	Invasive Mucinous Carcinoma	1
13	No Cancer Cells	N/A
14	No Cancer Cells	N/A

3.2 Multispectral image cubes of tissue before and after 2-NBDG incubation

Figure 1 represents the images acquired of both the malignant (IDC) and normal non-cancerous tissue before and after incubation with 2-NBDG. These two images are representative of the images analyzed from the malignant and normal tissues. The tumor specimen clearly showed brighter fluorescent signal after incubation with 2-NBDG (Fig. 1(b), T) as compared to its prestained image (Fig. 1(a), T) and the poststain image of the normal tissue (Fig. 1(b), N). Each tissue specimen had similarly low-levels of autofluorescence (Fig. 1(a)). The non-neoplastic tissue was mildly brighter after 2-NBDG incubation, which probably reflects the basal level of glucose uptake in normal tissue. Figure 1(c) illustrates a representative H&E stained tissue slice from the tumor specimen imaged in Fig. 1(b). It confirmed the presence of carcinoma in the tissue with high fluorescent signal.

Figure 1(d) illustrates the post stain image of a single specimen in which it was unknown whether there was presence of malignant tissue. This fluorescent image was used to slice the tissue into two different specimens, one that was believed to be cancerous and one that was non-cancerous. The presence of DCIS in the left-side aspect and normal tissue in the right-side aspect of the specimen was confirmed histologically.

#145022 - $15.00 USD Received 30 Mar 2011; revised 2 May 2011; accepted 10 May 2011; published 11 May 2011

3.3 Fluorescence spectra of tissue samples

The fluorescence spectra of the tissues imaged in Fig. 1(a) and 1(b) was calculated and is presented in Fig. 2. The spectra are representative of the spectra seen with the other tissues. The fluorescent signal of the malignant tissue after 2-NBDG staining was on average 13.1 ± 1.0 (average ± standard error of the mean) times greater at each wavelength than the signal calculated from the prestain image. Conversely, the fluorescence of normal breast tissue was only an average of 1.7 ± 0.1 times greater after addition of 2-NBDG. Hence, the fluorescence increase after 2-NBDG staining of the malignant tissue was much higher than that of the normal, non-cancerous control tissue, indicating that there was increased 2-NBDG consumption in the malignant tissue relative to the normal tissue.

Additionally, spectral analysis of the two different slices from Fig. 1(d) showed that the intensity at each wavelength was 2.0 ± 0.1 (data not shown) times greater in the malignant tissue than the normal tissue for each spectral measurement. This demonstrates that there was clear demarcation of an area of high fluorescence corresponding to DCIS and an adjacent low level of fluorescence corresponding to normal tissue.

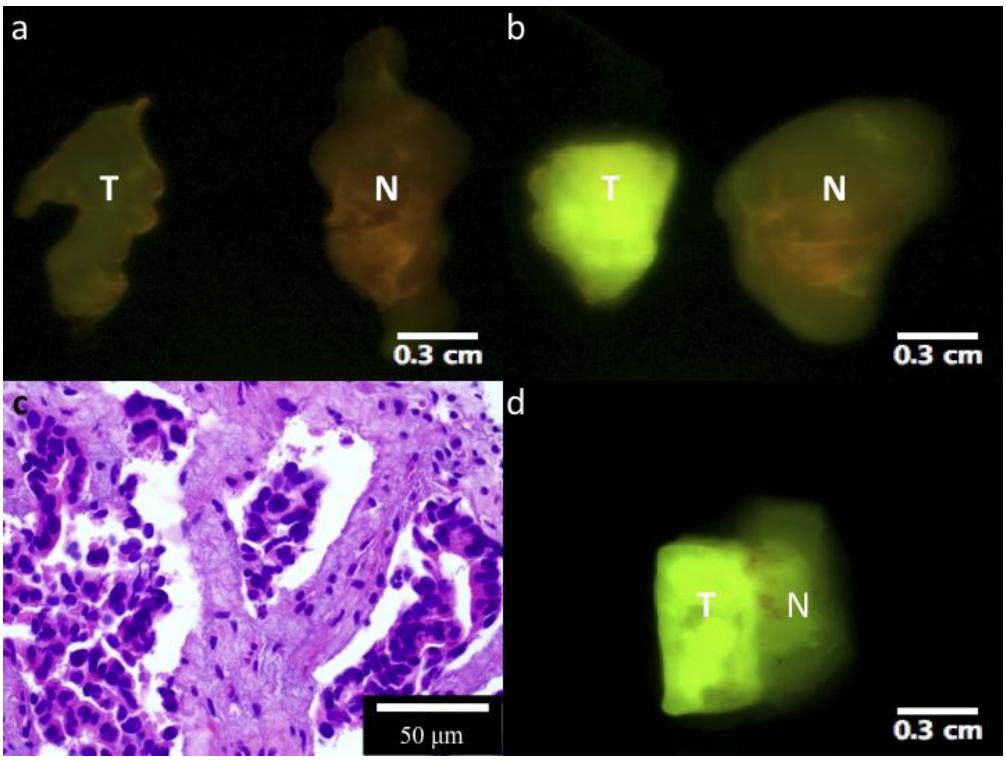

Fig. 1. Wide-field multispectral images of invasive ductal carcinoma (T) and normal breast tissue (N) from patient #6. (a) Tissues before being stained with 2-NBDG; (b) tissues after 2-NBDG staining. Tissues were excited with 445-490 nm light and images were collected after having passed through a 515 nm LP filter. (c) Tissue slice stained with hematoxylin and eosin depicts IDC. (d) One tissue slice with ductal carcinoma in situ (DCIS) and normal tissue. The left, brighter side was diagnosed as DCIS, whereas the other half was diagnosed as normal tissue.

One issue we addressed was if the intensity of 2-NBDG varied on a day-to-day basis. Our tests showed that the intensity variability at each wavelength was less than 3.2% of the average intensity calculated for each wavelength over the 4-day period; this demonstrated the system's stability and allowed us to perform quantitative analysis of the images.

#145022 - $15.00 USD Received 30 Mar 2011; revised 2 May 2011; accepted 10 May 2011; published 11 May 2011

The fluorescent signal difference between the poststain and prestain images from all the tumor samples and normal controls were averaged separately at each wavelength and are illustrated in Fig. 3. The difference in the intensity of fluorescence of the tumor samples was significantly higher than that of the normal controls at each wavelength from 520 to 720 nm (P<0.0001). At 580 nm (the center of the fluorescence spectrum peak ranging from 560 to 600 nm), the average intensity difference from the malignant tissues (1,878.2 ± 169.7) was 2.7 times higher than that from the normal non-cancerous tissue (704.9 ± 108.2).

To quantitatively distinguish the fluorescence of malignant tissue from that of normal, non-cancerous tissue, the NAUC values for the 560-600 nm range of the spectra were calculated for each sample (Fig. 4). The mean NAUC for the tumor samples (81,670 ± 7,142) was significantly higher than that for the control (31,170 ± 5,411, P<0.00001). The difference between malignant and non-cancerous tissue for some samples (#1, #5, and #10) exceeded a factor of 2; however, other tissues (#3, #6, #7, and #8) had less than a 2-fold difference between the tissues. The small differences did not seem to be limited to a particular type of breast cancer, as IDC had both some of the largest differences and some of the smallest differences. These differences can probably be attributed to each specific tissue and the part of the normal breast tissue that was provided by the pathologist.

Using the average NAUC (56,420) as a discrimination line, the NAUC values for nine of the malignant samples were above the line while the NAUC values for three were below. However, the NAUC value of all but one of the normal control samples was below the threshold.

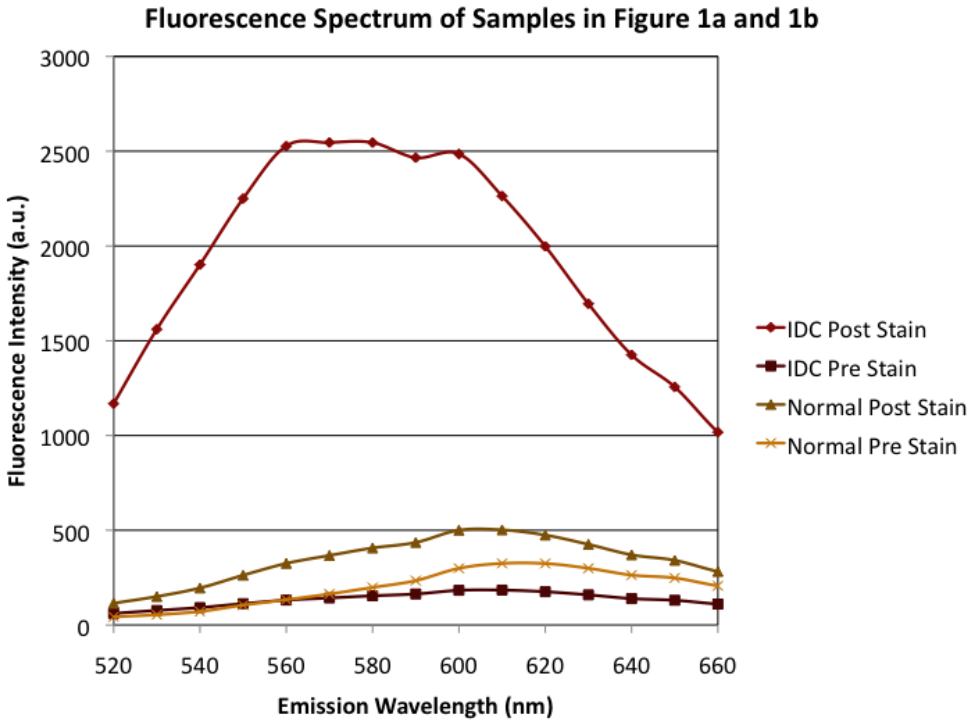

Fig. 2. Emission spectra of multispectral cubes represented in Fig. 1. Regions of interest were hand-drawn on each tissue; fluorescent signals every 10 nm from 520 to 660 nm are shown.

4. Discussion

The presence of positive surgical margins is associated with a higher risk of local disease relapse [3,16–18]. Typically, it is recommended that patients with positive margins on final

#145022 - $15.00 USD Received 30 Mar 2011; revised 2 May 2011; accepted 10 May 2011; published 11 May 2011

pathology undergo re-excision of the margins or intensification of adjuvant radiation therapy [19–21], both of which carry additional risks for the patients. Therefore, intraoperative evaluation of the surgical resection margins is an important component of the patient care. A rapid method of intraoperative margin evaluation could reduce second surgeries for breast cancer patients in the general community.

The study reported here represents an initial step towards the development of an optical imaging strategy that would aid both pathologists and surgeons in expediting the process of margin assessment during surgery. Our study demonstrates that 2-NBDG signal in tissue specimens can be analyzed both qualitatively and semi-quantitatively and that wide-field fluorescence imaging has the ability to discern malignant from normal tissue.

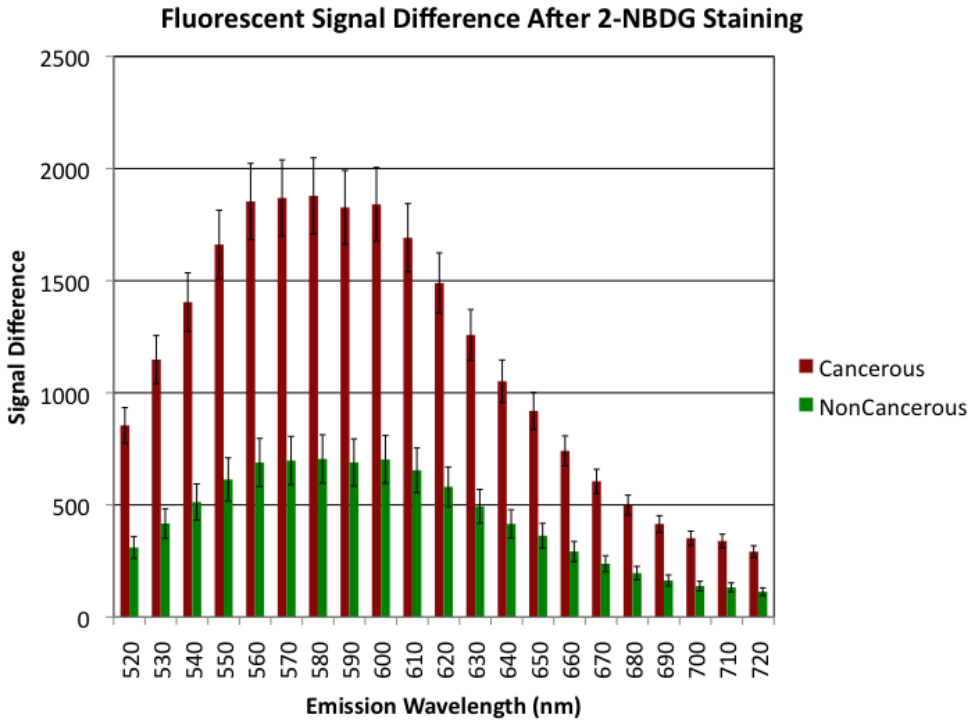

Fig. 3. Average signal difference between the poststain and prestain images calculated at each wavelength. A *t*-test comparison between the groups at each wavelength revealed that all of the groups were statistically different ($P<0.0001$). Error bars represent standard error of the mean.

Our strategy is based on the same principles that make PET scans so effective in the detection of breast cancer cells in patients. Similar to ^{18}FDG used in PET scan, 2-NBDG is a glucose analogue that is transported into cells via the GLUT1 and GLUT2 transporters [13]. It undergoes the same metabolic processes as ^{18}FDG [14]. Since cancer cells express higher levels of GLUTs and lower levels of glucuose-6-phosphatase that metabolizes the glucose than normal cells [8–12], both ^{18}FDG and 2-NBDG accumulate in the cancer cells [22]. This process allows PET imaging and fluorescent imaging of the cancer cells using nuclear ^{18}FDG and fluorescent 2-NBDG contrast agents.

Nitin et al. demonstrated that following topical placement of 2-NBDG, the fluorophore entered the cancerous cells in both tissue phantoms and excised oral neoplasia [15]; this demonstrated the ability of 2-NBDG to differentiate cancerous cells because of their high metabolic activity not because the different extracellular structures found in cancerous tissue allow for better 2-NBDG diffusion. As well O'Neil et al. demonstrated that 2-NBDG does enter breast cancer cells and at a much higher rate than for non-cancerous cells [14].

#145022 - $15.00 USD Received 30 Mar 2011; revised 2 May 2011; accepted 10 May 2011; published 11 May 2011

Using 2-NBDG as a topical contrast agent, we were able to optically discriminate freshly excised breast tissue that contained cancer cells from the normal surrounding tissue using our *ex vivo* imaging system. The single specimen with DCIS and normal tissue in Fig. 1(d) demonstrates how readily the area of tissue with cancer cells can be imaged by the fluorescence from 2-NBDG uptake compared to the adjacent normal tissue and displays the potential of imaging tissue at the margin. By quantifying the fluorescence signal through spectrum AUC, we were able to set a threshold level that identified 9 out of 12 tissues that contained cancerous cells. Hence, this strategy may be developed in the future into an automated staining and quantification system to expedite the intraoperative assessment of excised specimen of tumor margins. With further studies, this strategy could even potentially be implemented to assess cancer cells at the surgical margin *in vivo*.

Clinical studies had found ILC was associated with lower standard uptake values (SUV) [23] and a higher false-negative rate than IDC in PET imaging [8,24–27]. However, our study suggests that the ILC cells do accumulate glucose preferentially over normal surrounding tissue. We found all three cancerous tissues that contained ILC showed high fluorescence intensity after metabolizing 2-NBDG (Fig. 4). In fact, one had the largest NAUC. Most likely, the diffuse growth pattern of ILC does not concentrate the FDG signal high enough beyond the resolution limit of the PET imager to generate a high SUV. However, due to the small number of samples that contained ILC, this result should be interpreted with caution.

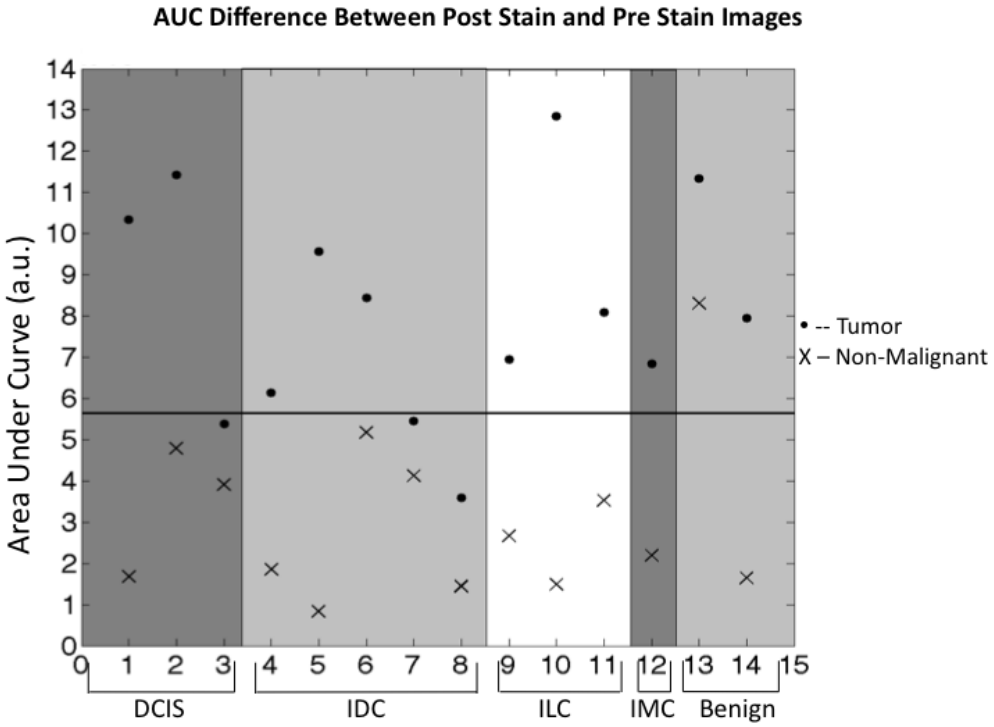

Fig. 4. Areas under each curve for the range of 560-600 nm. Each point on the graph represents the difference in AUC between the prestain and poststain images of the tissues from each patient. Dots represent the differences for tissues considered to be cancerous at time of collection. The black line represents the average NAUC of the two groups.

Similar to PET imaging, high basal metabolic state of the patient is likely to influence fluorescent glucose imaging of breast cancer. This most likely contributed to the high level of fluorescence in the normal breast tissue from patient #13 (Fig. 4). It was the only normal control tissue with NAUC above the threshold level. Likewise, the tumor sample obtained

#145022 - $15.00 USD Received 30 Mar 2011; revised 2 May 2011; accepted 10 May 2011; published 11 May 2011

from this patient also had high level of fluorescence although there were no cancer cells in the specimen. Therefore, similar to the steps implemented prior to the FDG-PET imaging in the clinics, the patients' metabolic state and glucose intake may need to be regulated to optimize the use of this strategy.

Further investigation of this strategy is required before it can be used in clinical settings. Foremost, this strategy is expected to have a minimal threshold limit of detection, and thus the minimum number of cancerous cells that can be detected by using the *ex vivo* imaging system needs to be determined. For this strategy to be clinically useful, it does not necessarily have to detect all margin tissue with cancer cells because the tissue would ultimately undergo permanent pathology review after the surgery, which would identify all cancer cells close or at the surgical margin. However, detection of cancer cells at the margin intraoperatively for some patients would spare those patients another surgical procedure for re-excision or adjuvant radiation treatment intensification.

In addition, the influence of breast cancer sub-types and treatments the patient received on the 2-NBDG uptake and imaging needs to be determined and optimized. In our study, patient #14 had received neoadjuvant chemotherapy with trastuzumab prior to her surgery. The tumor specimen from this patient had high fluorescence intensity but did not contain cancer cells. This elevated fluorescence level could be a result of the increase in immune response and activated natural killer cells that was reported in patients with breast cancer that overexpresses the human epidermal growth factor receptor 2 (HER2) and were treated with chemotherapeutic drugs [28,29]. This is an example of the many factors that need to be considered when considering this technology's clinical use.

In conclusion, this study represents the initial step towards the development of fluorescence imaging system that can improve diagnostic imaging in the clinic. Our goal was to develop a method that will optically differentiate malignant from non-cancerous tissue. Using this *ex vivo* wide-field imaging system, we were able to use a fluorescent glucose analogue and tunable light filters to create multispectral images that were analyzed to discriminate the presence of malignancy in excised tissue. Our future work includes optimizing an automated staining procedure so that this process can be an efficient and effective intraoperative tool for surgeons and pathologists.

Acknowledgments

We thank Nastassja Lewinski, Nadhi Thekkek, and Christine Wogan for editorial assistance; Sharon Rice, Laura Bales, Lisa Arriaga and the MD Anderson Breast Tumor Bank for providing tissue samples; the Breast Cancer Management System; and the Nelly B. Connally Breast Cancer Research Fund for its support of the Breast Tumor Bank and Breast Cancer Management System. We also thank Mr. and Mrs. Jon and Rebecca Brumley for their fund to support this research.

#145022 - $15.00 USD Received 30 Mar 2011; revised 2 May 2011; accepted 10 May 2011; published 11 May 2011